



**Time-lapse RGB  
imagery for a remote  
Greenlandic river**

C. J. Gleason et al.

This discussion paper is/has been under review for the journal Hydrology and Earth System Sciences (HESS). Please refer to the corresponding final paper in HESS if available.

# Technical Note: Semi-automated classification of time-lapse RGB imagery for a remote Greenlandic river

C. J. Gleason<sup>1</sup>, L. C. Smith<sup>1</sup>, D. C. Finnegan<sup>2</sup>, A. L. LeWinter<sup>2</sup>, L. H. Pitcher<sup>1</sup>, and V. W. Chu<sup>1</sup>

<sup>1</sup>Department of Geography, University of California – Los Angeles, 1255 Bunche Hall, 405 Hilgard Avenue, Los Angeles, California 90095-1524, USA

<sup>2</sup>US Army Cold Regions Research & Engineering Laboratory, Hanover, NH 03755, USA

Received: 30 November 2014 – Accepted: 14 January 2015 – Published: 29 January 2015

Correspondence to: C. J. Gleason (cjgleaso@ucla.edu)

Published by Copernicus Publications on behalf of the European Geosciences Union.

[Title Page](#)

[Abstract](#) [Introduction](#)

[Conclusions](#) [References](#)

[Tables](#) [Figures](#)

[◀](#) [▶](#)

[◀](#) [▶](#)

[Back](#) [Close](#)

[Full Screen / Esc](#)

[Printer-friendly Version](#)

[Interactive Discussion](#)



## Abstract

River systems in remote environments are often challenging to monitor and understand where traditional gauging apparatus are difficult to install or where safety concerns prohibit field measurements. In such cases, remote sensing, especially terrestrial time lapse imaging platforms, offer a means to better understand these fluvial systems. One such environment is found at the proglacial Isortoq River in southwest Greenland, a river with a constantly shifting floodplain and remote Arctic location that make gauging and in situ measurements all but impossible. In order to derive relevant hydraulic parameters for this river, two RGB cameras were installed in July of 2011, and these cameras collected over 10 000 half hourly time-lapse images of the river by September of 2012. Existing approaches for extracting hydraulic parameters from RGB imagery require manual or supervised classification of images into water and non-water areas, a task that was impractical for the volume of data in this study. As such, automated image filters were developed that removed images with environmental obstacles (e.g. shadows, sun glint, snow) from the processing stream. Further image filtering was accomplished via a novel automated histogram similarity filtering process. This similarity filtering allowed successful (mean accuracy 79.6 %) supervised classification of filtered images from training data collected from just 10 % of those images. Effective width, a hydraulic parameter highly correlated with discharge in braided rivers, was extracted from these classified images, producing a hydrograph proxy for the Isortoq River between 2011 and 2012. This hydrograph proxy shows agreement with historic flooding observed in other parts of Greenland in July 2012 and offers promise that the imaging platform and processing methodology presented here will be useful for future monitoring studies of remote rivers.

## HESSD

12, 1311–1327, 2015

### Time-lapse RGB imagery for a remote Greenlandic river

C. J. Gleason et al.

[Title Page](#)

[Abstract](#)

[Introduction](#)

[Conclusions](#)

[References](#)

[Tables](#)

[Figures](#)



[Back](#)

[Close](#)

[Full Screen / Esc](#)

[Printer-friendly Version](#)

[Interactive Discussion](#)



# 1 Introduction

Proglacial streams and rivers along land-terminating edges of the Greenland Ice Sheet are among the world's most difficult fluvial systems to study in the field, owing to their remoteness, harsh climate, and braided morphology. Discharge variations in large proglacial rivers are of particular scientific interest, as these systems typically derive water from the interior ablations surface Greenland Ice Sheet and are thus useful for inferring runoff mass losses from the ice sheet (Rennermalm et al., 2013; Smith et al., 2014). However, their high sediment loads, unstable banks, and dynamic braided channels present challenges to traditional in situ river gauging techniques, and long term hydrographs for these rivers are rare. While not unique to Greenland, these challenges are particularly evident there, with more than 100 large (> 1 km width) large braided rivers exiting the ice sheet with no observations of discharge whatsoever.

Where in situ methods are impractical, remotely sensed imagery offers an increasingly viable option for obtaining scientifically useful estimates of river discharge in remote or otherwise inaccessible areas (Smith et al., 1997; Ashmore and Sauks, 2006; Durand et al., 2010; Gleason and Smith, 2014). Braided rivers in particular typically display a power-law relationship between floodplain inundation area (which can be remotely sensed) and discharge, which has been exploited using satellites and terrestrial time-lapse photography (Smith, 1995, 1996; Chandler et al., 2002; Ashmore and Sauks, 2006; Egozi and Ashmore, 2008; Smith and Pavelsky, 2008; Bertoldi et al., 2009; Hundey and Ashmore, 2009; Bertoldi et al., 2010; Bird et al., 2010; Ashmore et al., 2011; Welber et al., 2012).

Regardless of the technology used, each remotely sensed image must first be classified into areas of water and non-water, a task for which numerous methodologies exist. In satellite remote sensing, NIR wavelengths can reliably detect open water surfaces. However, satellite imagery often lacks the required spatial and temporal resolution to adequately capture hydrologic phenomena, especially for smaller rivers. This has led to the use of non-metric, true color (RGB) digital camera imagery to capture water

## HESSD

12, 1311–1327, 2015

### Time-lapse RGB imagery for a remote Greenlandic river

C. J. Gleason et al.

[Title Page](#)

[Abstract](#)

[Introduction](#)

[Conclusions](#)

[References](#)

[Tables](#)

[Figures](#)



[Back](#)

[Close](#)

[Full Screen / Esc](#)

[Printer-friendly Version](#)

[Interactive Discussion](#)





parameter that has been shown to be highly correlated with discharge in braided rivers and has been successfully extracted from remotely sensed data in proglacial environments (Smith et al., 1996; Smith, 1997; Ashmore and Sauks, 2006; Smith and Pavelsky, 2008; Ashmore et al., 2011). To evaluate the robustness of the extraction, we assess image classification accuracy using manually generated ground truth data.

## 2 Data

This study was conducted on the proglacial Isortoq River in southwestern Greenland. The Isortoq, one of the largest braided rivers draining the Greenland ice sheet, issues from the Issunguata Sermia glacier terminus with discharge dominated by meltwater outflow from the ablating ice surface (Smith et al., 2014). In July 2011, two Nikon D200 model RGB cameras (focal lengths of 24 and 50 mm) were installed 250 m above a reach of the Isortoq braid plain approximately 3.1 km downstream of the ice edge. The camera system was identical to that developed by the Extreme Ice Survey project (www.extremeicesurvey.org) for use in severe Arctic conditions. In addition to the cameras, a modified battery pack and electronic controller were housed inside a weather-proof case with an abrasion-resistant viewing window. The case was mounted on a survey tripod and powered by a 12 V gel battery recharged by solar panel. The cameras were oriented so as to image sections of the braid plain of approximately 1.5 km × 2.0 km and 2.0 km × 2.3 km, respectively (Fig. 1), and captured one image every 30 min when light conditions permitted.

Camera data collection commenced 22 July 2011, and over 20 000 images were retrieved from the cameras by 10 September 2012, covering most of two melt seasons. The camera setup proved robust: the light sensor operated properly, the position of the cameras remained unchanged, and the batteries powering the cameras were still functional after the one year collection period for the wide focus camera. However, a presumed Arctic fox chewed through the cables connecting the battery to the camera for the more narrowly focused platform and halted data collection only two months after

### Time-lapse RGB imagery for a remote Greenlandic river

C. J. Gleason et al.

Title Page

Abstract

Introduction

Conclusions

References

Tables

Figures



Back

Close

Full Screen / Esc

Printer-friendly Version

Interactive Discussion



installation. Therefore, all analyses presented in this paper refer to the wide focus camera, which remained continuously operable throughout the study period 22 July 2011–10 September 2012.

### 3 Methods

Classifying the RGB image data into water and non-water areas to extract  $W_e$  presented several technical challenges for the 10327 images that were collected by the wide focus camera from July 2011 to September 2012. Existing approaches for hydraulic parameter extraction from RGB data require either manual or supervised classification of water within each image and are thus inappropriate for the large data volumes generated in this study. Unsupervised classification techniques provide a straightforward alternative for large time-lapse camera datasets, yet also present additional challenges as the images collected here are extremely diverse and differing soil moisture in the braid plain gives the appearance of multiple classes of output. Environmental factors such as time-varying solar angles, blowing sand, dense fog, shadowing, snow and rain on the camera lens, and acute sun-glint from water surface are especially prevalent in the Isortoq image data. These factors were all addressed, and  $W_e$  accurately extracted, by the processing workflow described below and presented in Fig. 2.

#### 3.1 Environmental filtering

The first task for extracting  $W_e$  was to filter the large amount of image data into those images that were most easily classified into water and non-water areas by eliminating images containing the environmental obstacles described above. Once images are classified, water area (and therefore  $W_e$ ) may be calculated. Several filters were developed to remove these poor quality images. First, images acquired during periods of non-flow (before and after melt season activity) were culled. Next, images with shad-

## Time-lapse RGB imagery for a remote Greenlandic river

C. J. Gleason et al.

[Title Page](#)

[Abstract](#)

[Introduction](#)

[Conclusions](#)

[References](#)

[Tables](#)

[Figures](#)



[Back](#)

[Close](#)

[Full Screen / Esc](#)

[Printer-friendly Version](#)

[Interactive Discussion](#)



**Time-lapse RGB  
imagery for a remote  
Greenlandic river**

C. J. Gleason et al.

[Title Page](#)[Abstract](#)[Introduction](#)[Conclusions](#)[References](#)[Tables](#)[Figures](#)[Back](#)[Close](#)[Full Screen / Esc](#)[Printer-friendly Version](#)[Interactive Discussion](#)

owing were culled by calculating the zenith and azimuth angles of the sun relative to the river plain. Through visual inspection of the image time series, zenith angles less than  $65^\circ$  and azimuth angles between degrees were found to produce shadows created by steep valley walls that prevented accurate classification (note valley walls, Figs. 1 and 2). Next, images that exhibited excessive sun glinting were removed. Sun glint was defined as when an image exhibited either a ratio of the 95th brightness percentile to the 5th brightness percentile greater than 1.8 or contained more than 1 % of pixels with brightness value greater than 215. This filter was necessary, as sun glint was observed both on open water and saturated sand, making distinction between these very different fluvial environments difficult (Fig. 2). Successful application of these winter, shadow, and sun glint filters culled 9487 images from the image time series, leaving 840 images free of environmental obstacles that still represented every day of the two melt seasons.

### 3.2 Similarity filtering

Even with these stringent filters, unsupervised classification was still unable to delineate water surfaces with satisfactory accuracy, and the number of images remaining was still too large for supervised classification to be feasible. As such, a semi-supervised classification approach was developed. To perform this classification, another image filtering was needed to find images that were similar enough to one another to share training data from a small sample of images in a supervised classification. The presence of dense fog, blowing sand, or cloudiness changes the brightness values of the imagery, so even images collected with identical solar geometry can be difficult to classify in an unsupervised manner. A similarity filter was developed that selected images that not only had similar solar geometry, but also had the same brightness and illumination and were all free of environmental obstacles not covered by the first filtering.

This similarity filtering was accomplished by calculating and comparing the histograms of each of the red, green, and blue bands for each image. Histograms of

brightness values that fell into 100 bins evenly spaced from 0 to 255 (reflectance values) were calculated for each band of each image. Using the same bins for each image ensured that cross comparison of images would not be affected by stretching of the image data. Once these histograms were generated, the RMSE between histogram counts per bin was computed in a band-by-band pairwise permutation, giving a per-image and per-band indication of the similarity of every image to each other image. These band-by-band RMSE values were then averaged to arrive at an overall measure of image similarity. This metric was used to identify the 20 % of the images that were most similar to each other, resulting in 168 images that were collected at similar sun angles without any environmental obstacles. In addition, the similarity filter also produced images that contained four basic elements: dark (non-sun lit, turbid) water, bright (sun lit or non-turbid) water, dark (wet) sand, and bright (dry) sand.

### 3.3 Georectification and classification

Once the final filtering of images was complete, images were cropped to exclude the wide upstream floodplain and georectified into ground coordinates using a 4th degree polynomial transformation implemented in ENVI v4.8 (Fig. 2). Eighty ground control points were manually extracted from a 2 m panchromatic World View 2 image acquired on 23 September 2011 (paired with a camera image collected 10 min later) and used to define the basis for the transformation. This warping polynomial was subsequently applied to all filtered images. After georectification, each image pixel had dimensions of 1 m by 1 m, an appropriate resolution for camera data collected at this scale. These georectified pixels allowed calculation of water surface area, and thus  $W_e$ , from the classified images.

To classify images into water and non-water areas for  $W_e$  extraction, training data representing four classes (dark water, bright water, dark sand, and bright sand) were manually collected from a random 10 % sample (16 images) of the similarity filtered images. The RGB statistics generated from these training polygons were applied to all images passing the similarity filtering and used to train a maximum likelihood su-

## HESSD

12, 1311–1327, 2015

### Time-lapse RGB imagery for a remote Greenlandic river

C. J. Gleason et al.

Title Page

Abstract

Introduction

Conclusions

References

Tables

Figures



Back

Close

Full Screen / Esc

Printer-friendly Version

Interactive Discussion





located where the image data provided complete bank to bank coverage and indicated by the magenta polygon in Fig. 2.

## 4.2 Extracted $W_e$ hydrograph

The  $W_e$  hydrograph shown in Fig. 4 is a proxy for discharge variations in the Isortoq River from 2011–2012. Gaps in the date record indicate that there were no images that passed filtering on those dates, even though images were acquired half hourly. This is a result of prolonged rain events, heavy fog, or strong winds that caused images to be non-similar during these days. Despite these gaps, the data record still provides near daily coverage, indicating that filtering did not substantially affect the temporal distribution of the output data. Of note is the large peak in  $W_e$  seen in July of 2012, coinciding with historic melting of the Greenland ice sheet (Hall et al., 2013; Tedesco et al., 2013) and destruction of the Watson River bridge in the town of Kangerlussuaq (Smith et al., 2014), located approximately 15 km south of the Isortoq River.

Figure 4 also reveals that the relative magnitude of  $W_e$  during this melt event was an order of magnitude greater than  $W_e$  in low flow stages. This shows that the Isortoq River behaves like other braided rivers with non-cohesive bed material, as its width adjusts rapidly to changing discharge. In addition, the peak  $W_e$  observed here corresponds to almost complete floodplain occupation by the river, highlighting the difficulty of installing traditional gauging equipment at this site.

## 5 Conclusions

This paper has demonstrated the efficacy of a fixed position RGB time-lapse camera platform for hydraulic parameter extraction for a large proglacial braided river in a remote area of Greenland. The operational camera delivered over 10 000 half hourly images in just over one year of collection, and demonstrated remarkable resilience in the Greenlandic winter. Such a platform is useful for extraction of multiple hydraulic pa-

# HESSD

12, 1311–1327, 2015

## Time-lapse RGB imagery for a remote Greenlandic river

C. J. Gleason et al.

Title Page

Abstract

Introduction

Conclusions

References

Tables

Figures

⏪

⏩

◀

▶

Back

Close

Full Screen / Esc

Printer-friendly Version

Interactive Discussion



rameters, including effective width ( $W_e$ ), a proxy for discharge variations. To fully realize this monitoring potential, the  $W_e$  variations extracted for each image could be calibrated with a rating curve built from intermittent field data.

The above accuracy assessments indicate that the semi-supervised classification method produced accurate and unbiased results. An accurately delineated water surface is necessary to preserve the fidelity of extracted hydraulic parameters. The processing techniques described in this paper fall short of completely automated processing, yet this paper does present an analysis protocol that achieves a consistent standard of classification from images that are automatically selected for ease of classification. Furthermore, the similarity filtering presented herein allows for supervised classification of numerous images from minimal training data, enabling long term hydrologic records to be maintained without onerous manual classification of imagery or photogrammetrically challenging DEM extraction.

*Acknowledgements.* This research was supported by the NASA Remote Sensing Theory initiative (grant NNX12AB41G), NASA Cryosphere Program (grant NNX11AQ38G) managed by Thomas Wagner, and NASA Earth and Space Sciences Fellowship NNX12AN32H. Field logistical support was provided by CH2M Hill Polar Field Services, the Kangerlussuaq International Science Station (KISS), and Air Greenland.

## References

- Ashmore, P. and Sauks, E.: Prediction of discharge from water surface width in a braided river with implications for at-a-station hydraulic geometry, *Water Resour. Res.*, 42, W03406, doi:10.1029/2005wr003993, 2006.
- Ashmore, P., Bertoldi, W., and Gardner, J. T.: Active width of gravel-bed braided rivers, *Earth Surf. Proc. Land.*, 36, 1510–1521, doi:10.1002/esp.2182, 2011.
- Bertoldi, W., Zanoni, L., and Tubino, M.: Planform dynamics of braided streams, *Earth Surf. Proc. Land.*, 34, 547–557, doi:10.1002/esp.1755, 2009.

# HESSD

12, 1311–1327, 2015

## Time-lapse RGB imagery for a remote Greenlandic river

C. J. Gleason et al.

[Title Page](#)

[Abstract](#)

[Introduction](#)

[Conclusions](#)

[References](#)

[Tables](#)

[Figures](#)



[Back](#)

[Close](#)

[Full Screen / Esc](#)

[Printer-friendly Version](#)

[Interactive Discussion](#)



## Time-lapse RGB imagery for a remote Greenlandic river

C. J. Gleason et al.

[Title Page](#)

[Abstract](#)

[Introduction](#)

[Conclusions](#)

[References](#)

[Tables](#)

[Figures](#)



[Back](#)

[Close](#)

[Full Screen / Esc](#)

[Printer-friendly Version](#)

[Interactive Discussion](#)



- Bertoldi, W., Zanoni, L., and Tubino, M.: Assessment of morphological changes induced by flow and flood pulses in a gravel bed braided river: the Tagliamento River (Italy), *Geomorphology*, 114, 348–360, doi:10.1016/j.geomorph.2009.07.017, 2010.
- Bird, S., Hogan, D., and Schwab, J.: Photogrammetric monitoring of small streams under a riparian forest canopy, *Earth Surf. Proc. Land.*, 35, 952–970, 2010.
- Chandler, J., Ashmore, P., Paola, C., Gooch, M., and Varkaris, F.: Monitoring river-channel change using terrestrial oblique digital imagery and automated digital photogrammetry, *Ann. Assoc. Am. Geogr.*, 92, 631–644, doi:10.1111/1467-8306.00308, 2002.
- Durand, M., Rodriguez, E., Alsdorf, D. E., and Trigg, M.: Estimating river depth from remote sensing swath interferometry measurements of river height, slope, and width, *IEEE J. Sel. Top. Appl.*, 3, 20–31, doi:10.1109/jstars.2009.2033453, 2010.
- Egozi, R. and Ashmore, P.: Defining and measuring braiding intensity, *Earth Surf. Proc. Land.*, 33, 2121–2138, doi:10.1002/esp.1658, 2008.
- Gilvear, D. J., Davids, C., and Tyler, A. N.: The use of remotely sensed data to detect channel hydromorphology; River Tummel, Scotland, *River Res. Appl.*, 20, 795–811, doi:10.1002/rra.792, 2004.
- Gleason, C. J. and Smith, L. C.: Toward global mapping of river discharge using satellite images and at-many-stations hydraulic geometry, *P. Natl. Acad. Sci. USA*, 11, 4788–4791, doi:10.1073/pnas.1317606111, 2014.
- Hall, D. K., Comiso, J. C., DiGirolamo, N. E., Shuman, C. A., Box, J. E., and Koenig, L. S.: Variability in the surface temperature and melt extent of the Greenland ice sheet. *Geophys. Res. Lett.*, 40, 2114–2120, doi:10.1002/grl.50240, 2013.
- Hundey, E. J. and Ashmore, P. E.: Length scale of braided river morphology, *Water Resour. Res.*, 45, W08409, doi:10.1029/2008wr007521, 2009.
- Rennermalm, A. K., Smith, L. C., Chu, V. W., Box, J. E., Forster, R. R., Van den Broeke, M. R., Van As, D., and Moustafa, S. E.: Evidence of meltwater retention within the Greenland ice sheet, *The Cryosphere*, 7, 1433–1445, doi:10.5194/tc-7-1433-2013, 2013.
- Smith, L. C.: Satellite remote sensing of river inundation area, stage, and discharge: a review, *Hydrol. Process.*, 11, 1427–1439, doi:10.1002/(SICI)1099-1085(199708)11:10<1427::AID-HYP473>3.0.CO;2-S, 1997.
- Smith, L. C. and Pavelsky, T. M.: Estimation of river discharge, propagation speed, and hydraulic geometry from space: Lena River, Siberia, *Water Resour. Res.*, 44, W03427, doi:10.1029/2007wr006133, 2008.

Smith, L. C., Isacks, B. L., Bloom, A. L., and Murray, A. B.: Estimation of discharge from three braided rivers using synthetic aperture radar satellite imagery: potential application to ungauged basins, *Water Resour. Res.*, 32, 2021–2034, doi:10.1029/96wr00752, 1996.

Smith, L. C., Chu, V. W., Yang, K., Gleason, C. J., Pitcher, L. H., Rennermalm, A. K., Legli-  
5 eter, C. J., Behar, A. E., Overstreet, B. T., Moustafa, S. E., Tedesco, M., Forster, R. R., LeWin-  
ter, A. L., Finnegan, D. C., Sheng, Y., and Balog, J.: Efficient meltwater drainage through  
supraglacial streams and rivers on the southwest Greenland ice sheet, *P. Natl. Acad. Sci.*  
USA, doi:10.1073/pnas.1413024112, in press, 2014.

Tedesco, M., Fettweis, X., Mote, T., Wahr, J., Alexander, P., Box, J. E., and Wouters, B.: Ev-  
10 idence and analysis of 2012 Greenland records from spaceborne observations, a regional  
climate model and reanalysis data, *The Cryosphere*, 7, 615–630, doi:10.5194/tc-7-615-2013,  
2013.

Welber, M., Bertoldi, W., and Tubino, M.: The response of braided planform configuration to  
15 flow variations, bed reworking and vegetation: the case of the Tagliamento River, Italy, *Earth*  
*Surf. Proc. Land.*, 37, 572–582, doi:10.1002/esp.3196, 2012.

# HESSD

12, 1311–1327, 2015

## Time-lapse RGB imagery for a remote Greenlandic river

C. J. Gleason et al.

[Title Page](#)

[Abstract](#)

[Introduction](#)

[Conclusions](#)

[References](#)

[Tables](#)

[Figures](#)



[Back](#)

[Close](#)

[Full Screen / Esc](#)

[Printer-friendly Version](#)

[Interactive Discussion](#)





**Figure 1.** Fig. 1 shows example images taken on 17 July 2012 of the Isortoq River by the two camera systems as well as the cameras themselves (foreground and background, **a**). The Issunguata Sermia Glacier is seen in the background, and nearly all water in this river is derived from its melting terminus. Only the wide focus camera (**c**) has a continuous data record from 2011–2012, as a presumed Arctic fox severed the wiring on the narrow focus camera. The yellow polygon in the wide focus image shows the target reach for  $W_e$  extraction, covering an area of approximately 1000 by 2000 m.

# HESSD

12, 1311–1327, 2015

## Time-lapse RGB imagery for a remote Greenlandic river

C. J. Gleason et al.

Title Page

Abstract

Introduction

Conclusions

References

Tables

Figures

◀

▶

◀

▶

Back

Close

Full Screen / Esc

Printer-friendly Version

Interactive Discussion



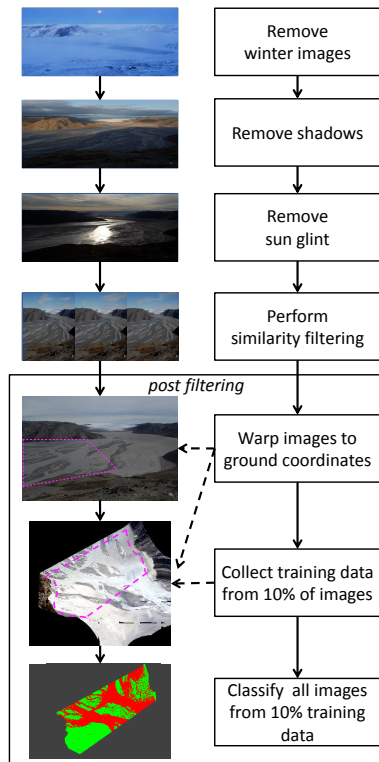


**Figure 2.** The processing steps required to extract  $W_e$  from raw images are shown here. Every step until the final classification is completely automated, allowing for a vast reduction in processing time. Winter images were selected by a manual inspection of first and last observed open water flow. Shadowing was defined as when solar zenith angles were less than  $65^\circ$  or solar azimuth between  $245\text{--}290$  or  $70\text{--}100^\circ$ , and sun glint was defined as a ratio of pixel brightness and as a total pixel value threshold. As Fig. 4 shows, these filters did not significantly affect the temporality of the data and almost every day during the two melt season study duration is represented.

**Time-lapse RGB imagery for a remote Greenlandic river**

C. J. Gleason et al.

Title Page

Abstract Introduction

Conclusions References

Tables Figures

◀ ▶

◀ ▶

Back Close

Full Screen / Esc

Printer-friendly Version

Interactive Discussion



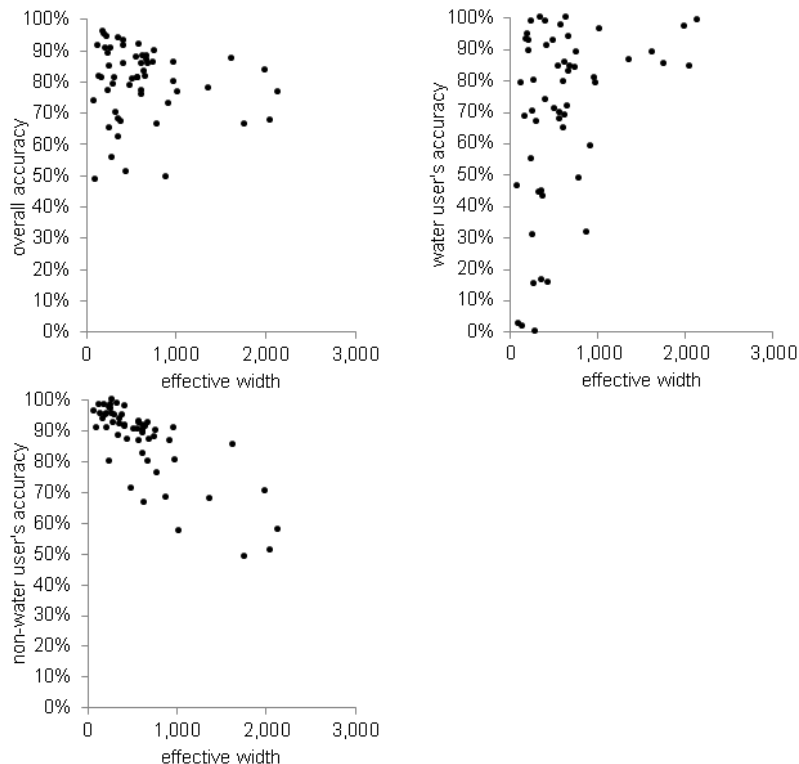


**Figure 3.** Accuracy assessment as a function of  $W_e$  from a 33% sample of post filtered images is presented here, with overall accuracy (a), water user's accuracy (b), and non-water user's accuracy (c) all showing acceptable performance. Overall accuracy and water user's accuracy are not strongly correlated with  $W_e$ , suggesting that the amount of water in the scene does not strongly influence the calculation of water area. Non-water accuracy, however, is strongly affected by the amount of water in the scene as the Isortoq River occupies nearly the entire valley at high flow, making classification of a few scattered non-water pixels challenging.

Time-lapse RGB  
imagery for a remote  
Greenlandic river

C. J. Gleason et al.

Title Page	
Abstract	Introduction
Conclusions	References
Tables	Figures
◀	▶
◀	▶
Back	Close
Full Screen / Esc	
Printer-friendly Version	
Interactive Discussion	



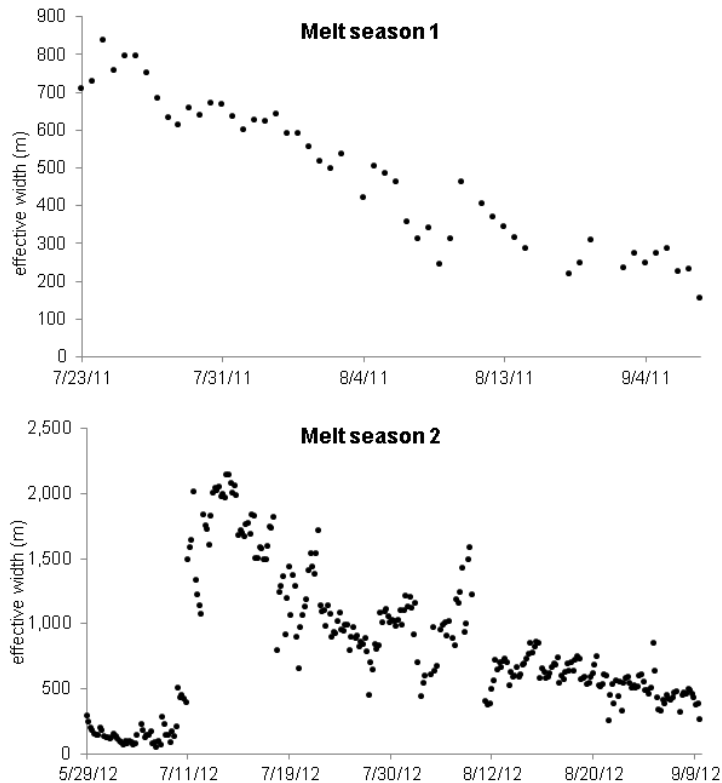


**Figure 4.** Successful image classification allowed for extraction of  $W_e$  across two melt seasons from the wide angle camera and gives a proxy for discharge in the braided Isortoq River. 22 statistical outliers, representing poorly classified images, were removed before generating this figure. These  $W_e$  time series clearly show historic flooding in Greenland in July of 2012, as well as the abrupt start of the 2012 melt season, and suggest that the camera platform and semi-automated classification techniques advanced here are sufficient for monitoring of this remote river.

**Time-lapse RGB imagery for a remote Greenlandic river**

C. J. Gleason et al.

Title Page

Abstract Introduction

Conclusions References

Tables Figures

◀ ▶

◀ ▶

Back Close

Full Screen / Esc

Printer-friendly Version

Interactive Discussion

